NANO LETTERS

pubs.acs.org/NanoLett

Can Graphene be used as a Substrate for Raman Enhancement?

Xi Ling,[†] Liming Xie,[†] Yuan Fang,[†] Hua Xu,[‡] Haoli Zhang,[‡] Jing Kong,[§] Mildred S. Dresselhaus,[§] Jin Zhang,*[,†] and Zhongfan Liu*[,†]

[†]Beijing National Laboratory for Molecular Sciences, Key Laboratory for the Physics and Chemistry of Nanodevices, State Key Laboratory for Structural Chemistry of Unstable and Stable Species, College of Chemistry and Molecular Engineering, Peking University, Beijing 100871, China, [‡]State Key Laboratory of Applied Organic Chemistry, College of Chemistry and Chemical Engineering, Lanzhou University, Lanzhou 730000, China, and [§]Department of Electrical Engineering and Computer Science, Massachusetts Institute of Technology, Cambridge, Massachusetts 02139

ABSTRACT Graphene is a monolayer of carbon atoms packed into a two-dimensional (2D) honeycomb crystal structure, which is a special material with many excellent properties. In the present study, we will discuss the possibility that graphene can be used as a substrate for enhancing Raman signals of adsorbed molecules. Here, phthalocyanine (Pc), rhodamine 6G (R6G), protoporphyin IX (PPP), and crystal violet (CV), which are popular molecules widely used as a Raman probe, are deposited equally on graphene and a SiO_2/Si substrate using vacuum evaporation or solution soaking. By comparing the Raman signals of molecules on monolayer graphene and on a SiO_2/Si substrate, we observed that the intensities of the Raman signals on monolayer graphene are much stronger than on a SiO_2/Si substrate, indicating a clear Raman enhancement effect on the surface of monolayer graphene. For solution soaking, the Raman signals of the molecules are visible even though the concentration is low to 10^{-8} mol/L or less. What's more interesting, the enhanced efficiencies are quite different on monolayer, few-layer, multilayer graphene, graphite, and highly ordered pyrolytic graphite (HOPG). The Raman signals of molecules on multilayer graphene are even weaker than on a SiO_2/Si substrate, and the signals are even invisible on graphite and HOPG. Taking the Raman signals on the SiO_2/Si substrate as a reference, Raman enhancement factors on the surface of monolayer graphene can be obtained using Raman intensity ratios. The Raman enhancement factors are quite different for different peaks, changing from 2 to 17. Furthermore, we found that the Raman enhancement factors can be distinguished through three classes that correspond to the symmetry of vibrations of the molecule. We attribute this enhancement to the charge transfer between graphene and the molecules, which result in a chemical enhancement. This is a new phenomenon for graphene that will expand the application of graphene to microanalysis and is good for studying the basic properties of both graphene and SERS.

KEYWORDS Graphene, Raman enhancement, substrate, vibrational symmetry

INTRODUCTION

Raman spectroscopy is an important and powerful tool in characterizing the structure of materials. However, due to the low scattering cross-section (10^{-30} cm^2 $molecule^{-1}$), the weak intensity of Raman signals result in low sensitivity, which is the reason why the application of Raman spectroscopy was neglected for many years.[1−3] The development of techniques for enhancing the Raman signals made Raman spectroscopy more popular in many kinds of research and applications.[4−9] The techniques are mainly based on resonant Raman scattering (RRS)[10] or surface-enhanced Raman scattering (SERS).[1,7,11] For RRS, the excitation wavelength should be resonant with a molecular transition. For surface-enhanced Raman spectroscopy (SERS), though there are numerous experimental and theoretical works on it, there are also many controversies about the mechanism and no complete picture of the enhancement mechanism is available even now.[12−23] Normally, the two widely accepted mechanisms are electromagnetic mechanism (EM) and chemical mechanism (CM).[1]

EM is based on the enhancement of the local electromagnetic field that results in a significant increase in the cross section of the Raman scattering. The contribution to the electromagnetic enhancement is mainly due to the surface plasmons excited by the incident light. The enhancement is roughly proportional to $|E|^4$ and can get to 10^8 or more, where E is the intensity of the electromagnetic field.[11,21] Compared to EM, CM[11,12,14] is based on a charge transfer between the molecule and the substrate. Because of charge transfer, the positive and negative charge in the molecule become more separated, which means the polarizability of the molecule increases, and then the cross section of the Raman scattering increases. CM is usually thought to be a "first layer effect". Some works show that the first monolayer of absorbed molecules often exhibits a SERS cross section much larger than that from the second layer.[11] The enhancement of CM is usually $10-10^2$. Additionally, EM is really a long-range effect that requires the substrate to be rough, so

* To whom correspondence should be addressed. Professor Jin Zhang, Center for Nanoscale Science and Technology (CNST), College of Chemistry and Molecular Engineering, Peking University, Beijing 100871, China. Telephone and Fax: 86-10-6275-7157. E-mail: jinzhang@pku.edu.cn (J.Z.); zfliu@pku.edu.cn (Z.L.).

Received for review: 10/13/2009
Published on Web: 12/29/2009

DOI: 10.1021/nl903414x | *Nano Lett.* **2010,** *10,* 553-561

that a so-called "hot spots" can exist between two particles, while CM is a short-range effect occurring on the molecular scale, which means it requires the molecule to be in contact with the substrate or very close to the substrate, so that charge transfer can easily occur between the molecule and the substrate. In many cases, the two mechanisms coexist. Usually, SERS is mostly based on EM including CM.

For SERS, the emphasis on getting strong enhancement is how to get a good substrate. Traditionally, the SERS substrate is based on a rough surface of a noble metal such as Ag, Au, Cu, and so on,[24,25] which takes advantage of the huge enhancement of EM compared to other enhancements. To make a rough metal surface for SERS, the following methods have been used: (1) electrochemical ways by successive oxidation−reduction cycles as in the work of Fleischmann and co-workers,[26] (2) depositing a thin film using vacuum evaporation methods,[27,28] (3) nanosphere lithography with the assistance of micro-nano-fabrication techniques,[29,30] (4) preparing size-controlled colloidal nanoparticles and depositing a monolayer on the substrate,[31−33] (5) assembling a large-area colloidal monolayer of nanoparticles on the substrate,[34] and so on. No matter which method is used, the fabrication process is relatively complex, difficult to control, reproduce, or keep clean, which leads to the low activity of SERS.[24] Also, the enhanced efficiency is often quite different for different metals. Silver is thought to be the best one, but it is expensive and easily oxidized, which will decrease the enhanced efficiency. Besides, metals usually have a bad biological compatibility. Therefore, it is necessary to develop new substrates for Raman enhancement. To satisfy further requirements, a material, which is cheap and easy to obtain, effective and can be used directly, chemically inert, and biocompatible should be exploited.

Graphene, a single sheet from graphite, has the ideal 2D structure with a monolayer of carbon atoms packed into a honeycomb crystal plane. Graphene is aromatic and hydrophobic and has great chemical inertness. People can get graphene by mechanical exfoliation from HOPG or Kish graphite. Graphite is abundant on the Earth's surface[35] and we can observe it by optical microscopy on a 300 nm thick SiO_2/Si substrate, which is cheap and convenient for most laboratories.[36−38] Also, it is biocompatible and has potential bioapplications.[39,40] As a rising star, it has attracted large interest from both physicists and chemists for its excellent properties both observed and predicted.[35,41−43] Actually, great progress has been made in finding applications for graphene, from chemical sensors to transistors.[44−47] Most of them are based on electrical measurements. But its potential as a substrate for Raman enhancement has not been investigated up to now. Here, we analyze the characteristics of classical SERS substrates first and then we consider whether graphene has potential as a substrate for Raman enhancement.

The EM mechanism requires a rough surface, metal particles with large curvature, and a surface that can absorb the incident light to produce surface plasmons. The CM mechanism requires the distance between the molecule and the substrate to be below 0.2 nm and the Fermi level of the metal substrate to symmetrically match with the highest occupied molecular orbital (HOMO) and lowest unoccupied molecular orbital (LUMO) of the molecule, so that charge transfer can occur from the metal to the molecule or vice versa.[1,14] Considering graphene, first, its surface is relatively smooth in despite of fluctuations that follow from the under lying substrate.[48] Second, the optical transmission through the graphene surface in the visible range is higher and is more than 95%.[49] Besides, the surface plasmon on graphene is in the range of terahertz rather than in the visible range.[50] On the basis of these considerations, graphene does not support EM. On the other hand, for CM graphene has possibilities. One of the most important conditions for CM is charge transfer between the molecule and the substrate. Since previous research has already shown that charge transfer could occur between graphene and some molecules,[51−54] we think that chemical enhancement may occur on the surface of graphene for selected molecules. In fact, in the earlier period, metals with a flat surface were used to separate CM from EM for further studying of the CM effect,[11] but the cold-deposited method that used to get a flat surface of a metal film is challenging since it requires very low temperature and ultrahigh vacuum. Graphene is an ideal 2D plane and the surface of graphene is quite flat. If graphene can be used as a substrate for Raman enhancement based on the chemical mechanism, it will provide an easy method to separate CM from EM for further study.

In this work, we use graphene as a substrate for Raman enhancement experiments. Some common molecules used for Raman probes, such as Pc, R6G, PPP, and CV are deposited equally on graphene and a SiO_2/Si substrate using vacuum evaporation or solution soaking. By comparing the Raman signals of molecules on monolayer graphene and on a SiO_2/Si substrate, we observed that the intensities of the Raman signals on monolayer graphene are much stronger than on the SiO_2/Si substrate. For solution soaking, we can observe Raman signals from the molecules on graphene even though the concentration is as low as 10^{-8} mol/L, while there is only a fluorescence background from the SiO_2/Si substrate that is consistent with our previous work.[55] Furthermore, the intensities decrease with an increase in the number of the layers of graphene and eventually the signals can no longer be seen on graphite and HOPG. The Raman enhancement factors of 2−17 are calculated by taking the signals on the SiO_2/Si substrate as references, and they are found to be dependent on the vibrational symmetry of the molecules. This is the first report about the Raman enhancement on the surface of graphene. Though the detailed origin is not so clear, we contribute this phenomenon to chemical enhancement due to the much easier charge transfer between graphene and the molecules. We believe that further

DOI: 10.1021/nl903414x | *Nano Lett.* **2010,** *10,* 553-561

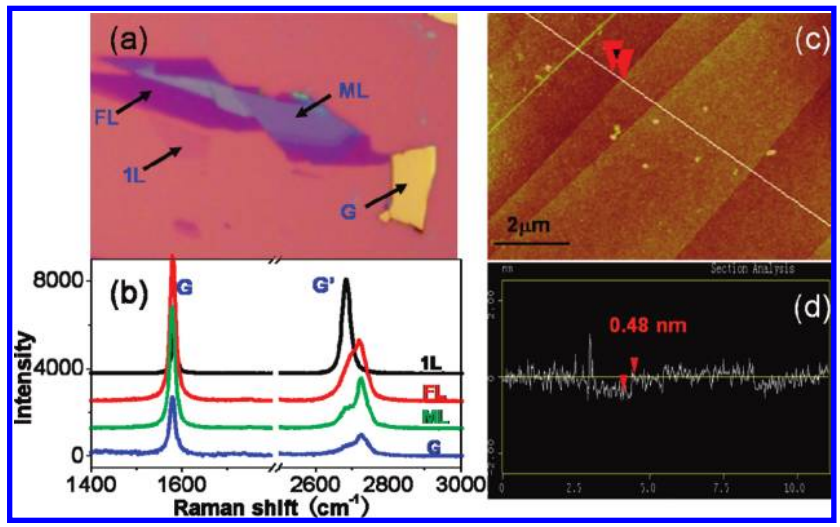

FIGURE 1. (a) The optical image of graphene, including single layer (1 L), few-layer (FL), multilayer (ML), and graphite (G). (b) The Raman spectra of different numbers of layers of graphene corresponding to (a). The data collection conditions are the same for all spectra. (c) The typical AFM image of graphene. (d) The cross-section analysis of (c).

research is needed in this direction to understand this special phenomenon.

EXPERIMENTAL SECTION

Graphene was prepared by the mechanical exfoliation of Kish graphite (Covalent Materials Corp.) using scotch tape on a SiO_2/Si substrate (300 nm thick oxide). Before graphene deposition, the SiO_2/Si substrate was washed clean by ultrasonication in acetone, ethanol, and water in turn, and at the end was cleaned by a Plasma Cleaner. Graphene was characterized by optical microscopy (OM), Raman spectroscopy, and atomic force microscope (AFM). By the color contrast in the OM image (Figure 1a), we can distinguish the relative number of layers as monolayer (1 L, pink), few-layer (FL, purple), multilayer (ML, purple close to white), and graphite (G, yellow). In this work, the number of layers is ~10 for FL, 50−100 for ML, and several hundred or more for graphite. The shape of the Raman G′-band and the $I_G/I_{G'}$ intensity ratio in the Raman spectra (Figure 1b) and the sample thickness in the AFM image (Figure 1c,d) can give more accurate information about the number of layers.

Phthalocyanine (Pc) from Alfa-Aesar, Rhodamine 6G (R6G) from Sigma-Aldrich, Protopphyrin IX (PPP) from Frontier Scientific, Inc., and Crystal Violet (CV) from Sinopharm Chemical Reagent Co., Ltd. were used directly as received. The chemical structures of these molecules are shown in the Supporting Information. The water used in this work is purified until the resistivity is 18.2 MΩ · cm.

We deposited the organic molecules on the surface of graphene using standard thermal evaporation. The pressure during the evaporation is about 10^{-4} Pa. The precision of the thickness measurement is 1 Å. Two kinds of thicknesses are used, 1 and 2 Å. For the sample deposited to 1 Å, we control the deposition time to about 3 s. For the thicknesses of 1 and 2 Å, the degrees of coverage are all less than a monolayer coverage as shown by many references.[56] The AFM images of graphene before and after molecular deposition also show a submonolayer coverage that the surface after deposition is as smooth as before (see Supporting Information Figure S2a−d). Meanwhile, for comparison, a bulk HOPG sample was put in the thermal evaporation system at the same time with the graphene sample. STM characterization also shows that the molecules on the surface form a submonolayer that we can only find when some molecules form a chain on the surface (see Supporting Information Figure S2e,f).

We also deposited the organic molecules on the surface of graphene by simply soaking the SiO_2/Si substrate with graphene in the solution of the molecules. Three kinds of molecules with a series of concentrations were used. One is a R6G solution (4×10^{-6}, 8×10^{-7}, 8×10^{-8}, 8×10^{-9}, 8×10^{-10}, 8×10^{-11} M in water); the second one is a PPP solution (2×10^{-5}, 2×10^{-6}, 2×10^{-7}, 1×10^{-7}, 5×10^{-8}, 2×10^{-8} M in methanol); the third one is a CV solution (1×10^{-6} M in water). The solutions with different concentrations were prepared by diluting the concentrated solution gradually. The soaking time is 1 h for all the solutions. After soaking, the sample with molecules was washed with the corresponding solvent to remove the free molecules and then dried under flowing N_2.

Raman spectroscopy was obtained using a Horiba HR800 Raman system with three laser lines, a 632.8 nm line from He−Ne laser, a 514.5 nm line from an Ar^+ laser (Spectra-Physics model 163-C4205), and a 457.9 nm line from an Ar^+ laser (Melles Griot model 543-AP-A01). The detector is a Synapse CCD detector with thermoelectric cooling to −70 °C. An 100× objective was used to focus the laser beam and to collect the Raman signal. The laser power on the sample was 0.5 mW for 632.8 nm, 0.2 mW for 514.5 nm, and 0.6mW for 457.9 nm to avoid possible heating effect by the

DOI: 10.1021/nl903414x | Nano Lett. 2010, 10, 553-561

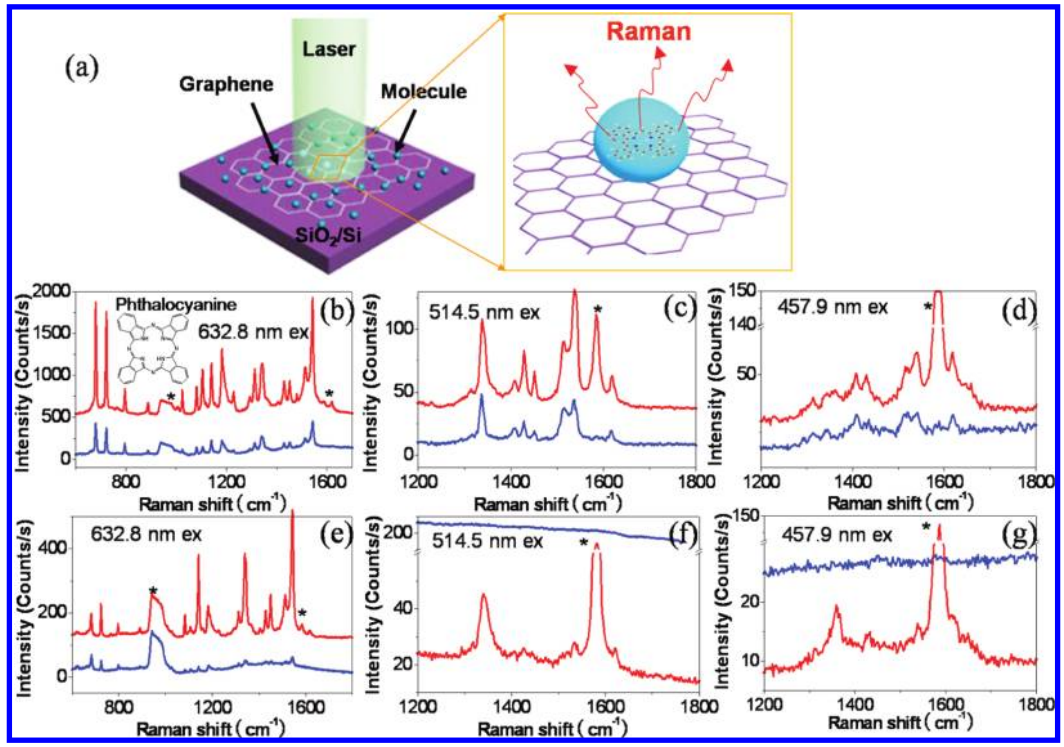

FIGURE 2. (a) Schematic illustration of the molecules on graphene and a SiO_2/Si substrate, and the Raman experiments. (b−d) are the comparisons of Raman signals of Pc deposited 2 Å on graphene (red line) and on the SiO_2/Si substrate (blue line) using vacuum evaporation at 632.8 nm excitation (b), 514.5 nm excitation (c), and 457.9 nm excitation (d). (e−g) Similar to (b−d), but depositing less Pc (~1 Å). Except for the peak marked by the star (*) (the 960 cm^{-1} peak from Si, and the 1586 cm^{-1} peak from graphene), all the peaks are from Pc. The inset in (b) shows the structure of Pc.

laser. The size of the laser spot is about 1 μm. The spectra in comparison were obtained under the same conditions. The intensities of the peaks are obtained by fitting them with a Lorentzian function.

RESULTS AND DISCUSSION

To investigate whether the graphene can be used as a substrate for Raman enhancement, submonolayer molecules were deposited on the sample by vacuum evaporation to ensure an equal distribution on the whole surface. First, the Raman signals of the molecules on graphene and on the SiO_2/Si substrate were compared. Pc with two kinds of thicknesses was deposited; one is thicker, about 2 Å and the other one is less, about 1 Å. Raman spectra were collected from both graphene and the SiO_2/Si substrate under the same conditions (integration time, laser power, focus, etc.). Figure 2a shows a schematic illustration of the molecules on graphene and on the SiO_2/Si substrate, and the results of the Raman experiment. We found that the signals of Pc on graphene are clearly stronger than that on the SiO_2/Si substrate, no matter which laser excitation was used (Figure 2). The assignments of the peaks are shown in the Supporting Information (Figure S3), which is in accordance with previous reports.[57,58] For the sample deposited at 2 Å Pc, Pc Raman signals were observed both on graphene and on the SiO_2/Si substrate at each wavelength excitation among 632.8 nm (Figure 2b), 514.5 nm (Figure 2c), and 457.9 nm (Figure 2d). We suppose that the absorption spectra of the molecules are not affected by the adsorption of the molecules, which has been shown to be very small by others.[59−61] The intensities of the Raman signals at 632.8 nm excitation are larger than at 514.5 and 457.9 nm, which is consistent with the fact that the absorption of Pc at 632.8 nm is much stronger than at 514.5 and 457.9 nm.[62] It is also interesting to note that the Raman signals of Pc on graphene are even stronger than the G-band of graphene (Figure 2b). In any case, the same trend is observed in all three cases and that the signals on graphene are stronger than that on the SiO_2/Si substrate. As the thickness of Pc on the surface decreases to 1 Å, the differences of the signals on graphene and on the SiO_2/Si substrate become even larger. At 632.8 nm excitation, which is better resonant with Pc, only very weak signals from Pc are observed on the SiO_2/Si substrate, while on graphene the signals are much stronger and well-distinguished (Figure 2e). At 514.5 and 457.9 nm excitation, which are outside the absorption range of Pc, the Raman signals at 1340, 1543, and 1617 cm^{-1} are still distinguishable on monolayer graphene, in contrast to the signals from Pc on the SiO_2/Si substrate, which are invisible and only the fluorescence background can be seen (Figure 2f,g). In Figure 2f,g, the baselines for graphene and the SiO_2/Si substrate are not at the same level, which is due to the graphene-induced fluorescence quenching.[55]

DOI: 10.1021/nl903414x | *Nano Lett.* **2010,** *10,* 553-561

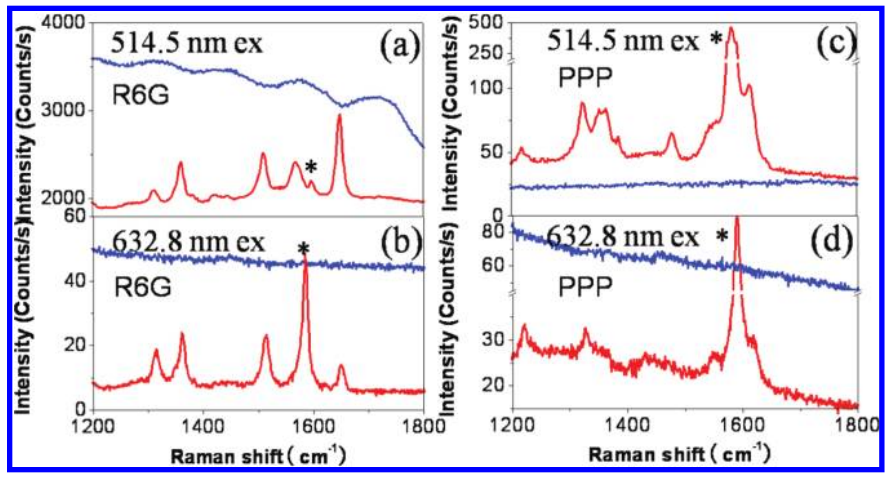

FIGURE 3. Comparisons of Raman signals of R6G and PPP deposited on graphene (red line) and on the SiO_2/Si substrate (blue line) using vacuum evaporation at 514.5 nm excitation and 632.8 nm excitation. (a,b) R6G, (c,d) PPP. (a,c) Excitation at 514.5 nm. (b,d) Excitation at 632.8 nm. The peak marked by the star (*) is the G-band of graphene.

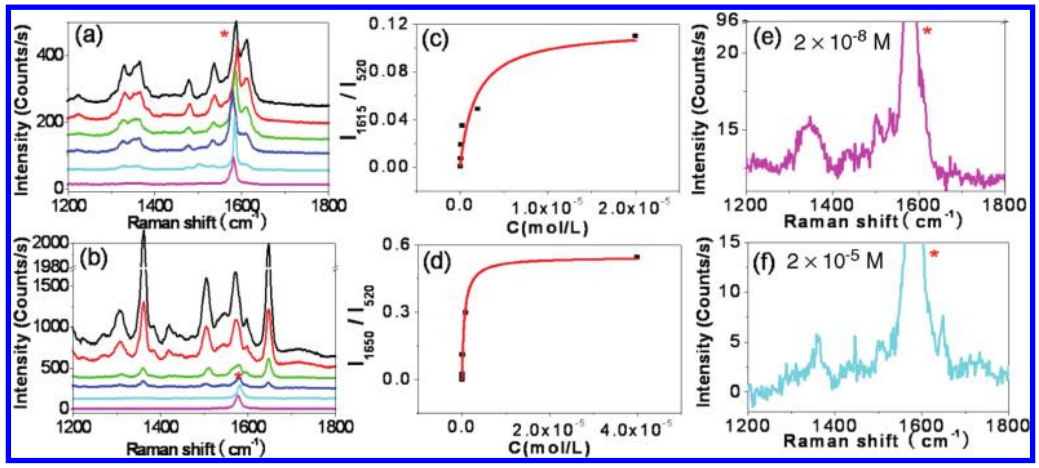

FIGURE 4. Raman spectra of PPP (a) and R6G (b) deposited on monolayer graphene by soaking in the solution with different concentrations. For PPP, the concentrations from top to bottom are 2×10^{-5}, 2×10^{-6}, 2×10^{-7}, 1×10^{-7}, 5×10^{-8}, and 2×10^{-8} M. For R6G, the concentrations from top to bottom are 4×10^{-5}, 8×10^{-7}, 8×10^{-8}, 8×10^{-9}, 8×10^{-10}, and 8×10^{-11} M. (c,d) The corresponding plots of Raman intensity vs concentration. For PPP, we choose the 1615 cm^{-1} peak as an example, and for R6G we choose the 1650 cm^{-1} peak. The intensities of the peaks are normalized to the signal from silicon at 520 cm^{-1}. (e,f) The magnified spectra of PPP under 2×10^{-8} M and R6G under 2×10^{-5} M, respectively. All the spectra are obtained at 514.5 nm excitation. The peak marked by the star (*) is the G-band of graphene.

The situation is similar for R6G and PPP deposited at about 1 Å. The assignments of the peaks of R6G and PPP are shown in the Supporting Information (Figure S3). At the resonant wavelength excitation of R6G (Figure 3a) and PPP (Figure 3c), 514.5 nm,[63−65] the spectra with strong Raman signals and high signal-to-noise ratio were observed on graphene, while only the fluorescence background was observed when collecting Raman spectra from the SiO_2/Si substrate. At the nonresonant wavelength excitation of R6G (Figure 3b) and PPP (Figure 3d), 632.8 nm, there is only a fluorescence background from the SiO_2/Si substrate as we expected, but on graphene, though the signal-to-noise ratio is not so good as for the 632.8 nm excitation, the signals from the molecules are still visible, which is interesting and exciting. What is more important is that even though the absorption is near to zero at 632.8 nm for R6G,[63] some signals such as 1312, 1360, 1512, and 1650 cm^{-1} from R6G appeared unexpectedly.

For further investigation, solution soaking was used to deposit the molecules. The detailed description about the solution soaking was mentioned in the experimental section. The samples were soaked in a PPP solution with six concentrations from 2×10^{-5} to 2×10^{-8} M and in a R6G solution with six concentrations from 4×10^{-5} to 8×10^{-11} M. The intensities of the Raman signals of the molecules on monolayer graphene decrease with a decrease in the concentration for both molecules (Figure 4a,b). The data can be fit well with the BET model (Figure 4c,d) and it is clear to see the intensity of the Raman signal saturate as the concentration is increased. So, under low concentrations, such as below 8×10^{-7} M for R6G and 2×10^{-6} M for PPP, the degrees of coverage can be thought to be submonolayer.

DOI: 10.1021/nl903414x | Nano Lett. 2010, 10, 553-561

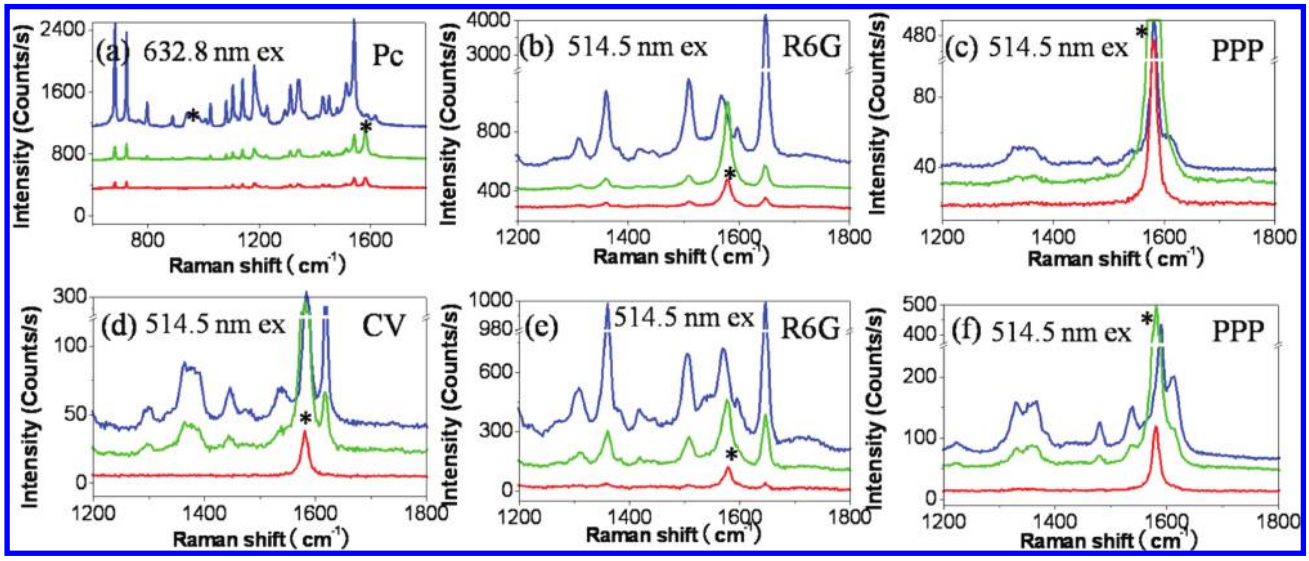

FIGURE 5. Raman spectra of Pc (a), R6G (b), and PPP (c) deposited using vacuum evaporation and the Raman spectra of CV (d), R6G (e), and PPP (f) deposited by solution soaking on different surfaces, respectively. The blue line is for spectra obtained on monolayer graphene, the green line is for spectra obtained on multilayer graphene, and the red line is for spectra obtained on graphite. In (e), the spectra are the results after removing the fluorescence background. For all the peaks, except the peaks marked by the star (*), all the peaks are from the indicated molecules.

More importantly, some signals from the molecules can be observed even for concentrations as low as 8×10^{-10} M for R6G (Figure 4e), and 2×10^{-8} M for PPP (Figure 4f). The concentration is comparable with the concentration used in the classical SERS experiments.[66,67] Compared to the situation on graphene, under all the concentrations both for R6G and PPP no Raman signals were observed on the SiO_2/Si substrate except the fluorescence background, which is the same as in our previous work.[55]

From the experimental data shown above, the much stronger Raman signals of the molecules on graphene compared with that on the SiO_2/Si substrate, and the appearance of the Raman signals for molecules on graphene when soaking in solutions with very low concentrations clearly suggests that a Raman enhancement effect exists on the surface of graphene. As a result of the Raman enhancement on the surface of graphene, we can obtain the Raman signals from very few molecules. Also, we can obtain Raman spectra from the molecules at nonresonant wavelength excitations to avoid the fluorescence background that sometimes occurs at resonant wavelength excitations.

Considering the origin of this special Raman enhancement on graphene, as mentioned in the introduction, EM is not likely, while CM is possible. First, the molecules we used are conjugated and macrocyclic (for Pc and PPP). Their basic structures are similar to graphene. When deposited as a submonolayer on graphene, due to the $\pi-\pi$ stacking, these aromatic molecules should lie parallel to the surface of graphene,[68−70] which means that the distance between graphene and the molecules is small. Second, the position of the HOMO and LUMO of the molecules are all located on the two sides of the Fermi level of graphene (see Supporting Information Figure S4.). These observations suggest that charge transfer can easily occur between graphene and the molecules, which will induce chemical enhancement. Additionally, because of the similarity of the chemical structure between the molecules and graphene, the vibrational coupling[71] between them may be another factor contributing to the Raman enhancement.

Under resonant excitation, the signals are attributed to three factors, the number of the molecules, resonant enhancement, and chemical enhancement. When the amount of molecules is small, the resonant enhancement is insufficient to observe the Raman signals of molecules, and there is no chemical enhancement on the SiO_2/Si substrate, and we cannot see the signals. But on graphene, both resonant enhancement and chemical enhancement exist, which result in observable Raman signals. At the nonresonant wavelength excitation, the signals are attributed to the number of molecules and to chemical enhancement. Because of the fewer molecules and no chemical enhancement on the SiO_2/Si substrate, no signals are observed, while on graphene chemical enhancement still exists, which results in a survival of the signals.

Then, to understand the Raman enhancement on graphene further, we compared the Raman signals of molecules on the surface of graphene with different numbers of layers. Figure 5 shows the Raman spectra of different molecules on monolayer (blue line), multilayer (green line), and graphite (red line), where molecules were deposited using both vacuum evaporation and solution soaking. For the samples deposited at 1 Å thickness by vacuum evaporation (Figure 5a−c), at the corresponding resonant wavelength excitation of Pc, R6G, and PPP, the intensities of the Raman signals from the corresponding molecules decrease with an increase of the number of graphene layers. On the graphite, the

DOI: 10.1021/nl903414x | *Nano Lett.* **2010,** *10,* 553-561

signals are usually very weak or invisible. On the surface of HOPG upon which molecules were deposited at the same time with the sample, the signals are hardly observed (see Supporting Information Figure S5.). The trend is analogous to that observed for the samples with deposited molecules obtained by solution soaking (Figure 5d−f). In ref 72, Wang et al. considered the incident laser and scattered Raman signal interference in between the graphene layers and in this way they explained the G band intensity dependence on the graphene layer number. However, if we apply the same consideration to our system here, we would expect the enhancement factors to oscillate periodically with the graphene thickness. Thus we conclude that the interference effect induced by the different numbers of graphene layers does not make a major contribution to the observed intensity.[72]

Regarding the difference of the Raman signals on monolayer and on multilayer graphene, though we do not know the precise origin of these signals, one possibility is the difference of the surface potential induced by the substrate-induced effects.[73] The p-doing effect from the SiO_2/Si substrate will result in an increase in the work function of graphene sheets with thickness, which may affect the efficiency of the chemical enhancement. Further work should be done to investigate the origin of this effect.

In order to calculate the Raman enhancement factors, we chose the intensity of the Raman signals of Pc on the SiO_2/Si substrate as the normalization reference. The data used here is at 632.8 nm wavelength excitation. In Figure 6, we show the relative intensities of 15 peaks of Pc on different numbers of layers of graphene. Comparing the signals from monolayer graphene with those from the SiO_2/Si substrate, we observed that the Raman enhancement factors of different peaks are different and vary from 2 to 17. According to the magnitude of the enhancement, the peaks are clearly distinguished into three classes. The peaks at 1140, 1340, 1450, 1512, and 1542 cm^{-1}, assigned as A_g symmetry vibrations,[74] are enhanced the most by about 15 times. The peaks at 1082, 1182, 1189, 1312, and 1428 cm^{-1}, assigned as B_{3g} modes, are enhanced by about 5 times,[74] and the peaks at 680, 722, 797, 890, and 1228 cm^{-1}, usually assigned as macrocycle breathing vibrations,[74,75] are enhanced relatively less, by about only 2 times. Also, there are some new peaks appearing, such as 766, 1159, 1405, 1479, and 1617 cm^{-1} (see Figure 2e, and the magnified spectra are shown in Supporting Information Figure S7). Most of them are assigned as E modes, which are infrared active (such as 766, 1159, and 1405 cm^{-1}),[57,74] whose intensity is usually weak in other SERS experiments.[58] Besides, because of the enhancement some overtones in the range 1800∼3400 cm^{-1} are visible (see Supporting Information Figure S8). This classification of the enhancement factors indicates a vibration symmetry dependence of the Raman enhancement for this effect. On the other hand, with an increase in the number of graphene layers the signals become weaker and

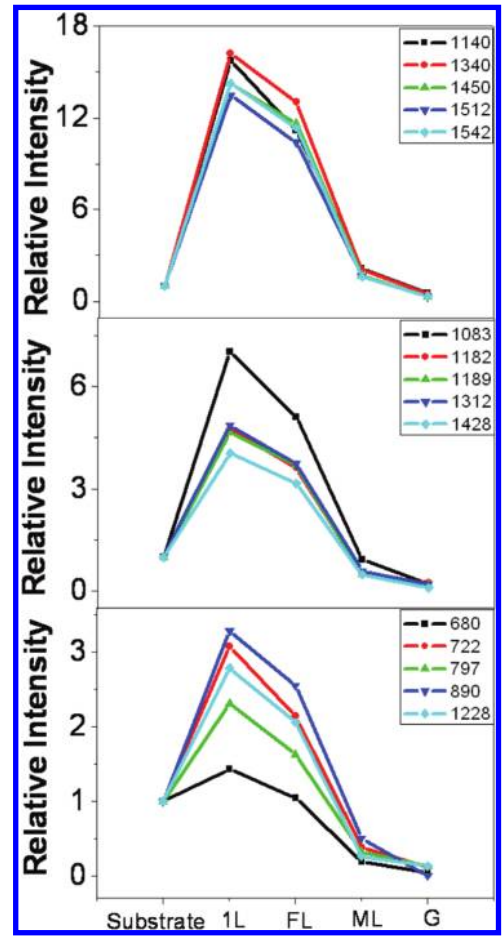

FIGURE 6. The relative Raman intensity of Pc deposited 1 Å on different surfaces using vacuum evaporation. The different spectral lines represent the different peaks of Pc labeled in the right top corner. The signals on the SiO_2/Si substrate are set to "1".

weaker. For few-layer graphene, the biggest enhancement factor is about 12. For multilayer and more layer graphene, the signals are even weaker than that on the SiO_2/Si substrate (Figure 6).

It should be noted that the magnitude of the enhancement, 2−17 times and the vibration dependence of the enhancement factors are both consistent with the chemical enhancement mechanism. For chemical enhancement, the enhancement of different vibrational modes is usually dependent on the geometry of the molecules on the surface.[76,77] Here, the enhancement in our system is also vibration dependent, which is related with the surface geometry of the molecule on graphene. The appearances of some new peaks may be due to symmetry-breaking of the molecule. Regarding the vibration dependence of the enhancement of the molecular signal with different vibrational modes and different orientations on the graphene, further investigations are being carried out in our group. These are expected to determine the geometry of the molecule on the surface of graphene by the difference in the Raman enhancement factors for different symmetry vibrations.

DOI: 10.1021/nl903414x | *Nano Lett.* **2010,** *10,* 553-561

In summary, in this study we discussed whether graphene can be used as a substrate for Raman enhancement. To investigate and understand this, a series of experiments were carried out. Two methods, vacuum evaporation and solution soaking, were used to deposit submonolayer molecules on graphene as well as on the SiO_2/Si substrate. First, the Raman signals of the molecules on monolayer graphene and on the SiO_2/Si substrate were compared and the Raman signals on monolayer graphene could be observed easily and were stronger than that on the SiO_2/Si substrate, indicating a clear Raman enhancement effect on the surface of monolayer graphene. Especially, for solution soaking the Raman signals of the molecules on graphene were visible even though the concentration was low and was comparable with the concentration used in the classical SERS experiment. Furthermore, the Raman enhancement effect was investigated on different layers graphene. The enhanced efficiency was found to be best on monolayer graphene (or few layer graphene, which needs further research). The intensities of the Raman signals of molecules decreased roughly with the increase of the number of the graphene layers. Since the precise origin is unknown, further investigations should be carried out. Finally, a Raman enhancement factor of 2−17 was obtained and the magnitude was found to be dependent on the vibrational symmetry of the modes of the molecules. Considering the discussion in the introduction and the results from the experimental data, we attribute this Raman enhancement in graphene to a chemical enhancement effect.

This is the first report about the Raman enhancement on the surface of graphene. Compared to metals, graphene as a substrate for Raman enhancement has many advantages such as easier preparation, lower cost, and better biocompatibility. Although the precise origin is not very clear now and more research should be carried out in this new research direction, we believe this discovery will expand the application of graphene to microanalysis and is good for the studying the basic properties of both graphene and SERS, such as the charge transfer of graphene and chemical enhancement mechanism, separating it from the electromagnetic enhancement mechanism.

Acknowledgment. This work was supported by NSFC (50972001, 20725307, and 50821061) and MOST (2006CB932701, 2006CB932403, and 2007CB936203). M.S.D. was supported by U.S. NSF DHR Grant 07-021197.

Supporting Information Available. Chemical structures of Pc, R6G, PPP, and CV, SPM characterization of the sample before and after deposition, the assignments of the peaks of Pc, R6G, PPP and CV, the relative position of the HOMO and LUMO of the molecules and the Fermi level of graphene, the Raman signals of R6G on HOPG, The magnified spectra of Figure 2(b),and the Raman spectra of Pc from 1800 cm^{-1} to 3400 cm^{-1}.This material is available free of charge via the Internet at http://pubs.acs.org.

REFERENCES AND NOTES

(1) Campion, A.; Kambhampati, P. *Chem. Soc. Rev.* **1998**, *27*, 241.
(2) *Raman Spectroscopy for Chemical Analysis*; McCreery, R. L., Ed.; Wiley-Interscience: New York, 2000.
(3) Pettinger, B. Chapter 6. In *Adsorption of Molecules at Metal Electrodes*; Lipkowski, J., Ross, P. N., Eds.; VCH: New York, 1992; p 285.
(4) Brolo, A. G.; Irish, D. E.; Smith, B. D. *J. Mol. Struct.* **1997**, *405*, 29.
(5) Cotton, T. M.; Kim, J. H.; Chumanov, G. D. *J. Raman Spectrosc.* **1991**, *22*, 729.
(6) Clark, R. J. H.; Dines, T. J. *Angew. Chem., Int. Ed. Engl.* **1986**, *25*, 131.
(7) Moskovits, M. *J. Raman Spectrosc.* **2005**, *36*, 485.
(8) Petry, R.; Schmitt, M.; Popp, J. *ChemPhysChem* **2003**, *4*, 14.
(9) Vodinh, T. *Sens. Actuators, B* **1995**, *29*, 183.
(10) Efremov, E. V.; Ariese, F.; Gooijer, C. *Anal. Chim. Acta* **2008**, *606*, 119.
(11) Otto, A.; Mrozek, I.; Grabhorn, H.; Akemann, W. *J. Phys: Condens. Matter* **1992**, *4*, 1143.
(12) Persson, B. N. J.; Zhao, K.; Zhang, Z. Y. *Phys. Rev. Lett.* **2006**, *96*, 207401.
(13) Persson, B. N. J.; Zhao, K.; Zhang, Z. Y. *Phys. Rev. Lett.* **2006**, *97*, 199702.
(14) Otto, A. *J. Raman Spectrosc.* **2005**, *36*, 497.
(15) Mrozek, I.; Otto, A. *J. Electron Spectrosc.* **1990**, *54*, 895.
(16) Le Ru, E. C.; Etchegoin, P. G. *Phys. Rev. Lett.* **2006**, *97*, 199701.
(17) Hildebrandt, P.; Keller, S.; Hoffmann, A.; Vanhecke, F.; Schrader, B. *J. Raman Spectrosc.* **1993**, *24*, 791.
(18) Wu, D. Y.; Liu, X. M.; Duan, S.; Xu, X.; Ren, B.; Lin, S. H.; Tian, Z. Q. *J. Phys. Chem. C* **2008**, *112*, 4195.
(19) Kovacs, G. J.; Loutfy, R. O.; Vincett, P. S.; Jennings, C.; Aroca, R. *Langmuir* **1986**, *2*, 689.
(20) Brown, R. J. C.; Wang, J.; Tantra, R.; Yardley, R. E.; Milton, M. J. T. *Faraday Discuss.* **2006**, *132*, 201.
(21) Schatz, G. C.; Young, M. A.; Van Duyne, R. P. *Top. Appl. Phys.* **2006**, *103*, 19.
(22) Otto, A.; Futamata, M. *Top. Appl. Phys.* **2006**, *103*, 147.
(23) Sun, M. T.; Liu, S. S.; Chen, M. D.; Xu, H. X. *J. Raman Spectrosc.* **2009**, *40*, 137.
(24) Lin, X. M.; Cui, Y.; Xu, Y. H.; Ren, B.; Tian, Z. Q. *Anal. Bioanal. Chem.* **2009**, *394*, 1729.
(25) Ren, B.; Liu, G. K.; Lian, X. B.; Yang, Z. L.; Tian, Z. Q. *Anal Bioanal Chem* **2007**, *388*, 29.
(26) Fleischm, M.; Hendra, P. J.; Mcquilla, Aj. *Chem. Phys. Lett.* **1974**, *26*, 163.
(27) Rowe, J. E.; Zwemer, D. A.; Murray, C. A.; Shank, C. V. *Abstracts of Papers of the American Chemical Society* **1980**, *180*, 77.
(28) Taylor, C. E.; Pemberton, J. E.; Goodman, G. G.; Schoenfisch, M. H. *Appl. Spectrosc.* **1999**, *53*, 1212.
(29) Jensen, T. R.; Malinsky, M. D.; Haynes, C. L.; Van Duyne, R. P. *J. Phys. Chem. B* **2000**, *104*, 10549.
(30) Hulteen, J. C.; Treichel, D. A.; Smith, M. T.; Duval, M. L.; Jensen, T. R.; Van Duyne, R. P. *J. Phys. Chem. B* **1999**, *103*, 3854.
(31) Creighton, J. A.; Blatchford, C. G.; Albrecht, M. G. *J. Chem. Soc., Faraday Trans. 2* **1979**, *75*, 790.
(32) Emery, S. R.; Haskins, W. E.; Nie, S. M. *J. Am. Chem. Soc.* **1998**, *120*, 8009.
(33) Krug, J. T.; Wang, G. D.; Emory, S. R.; Nie, S. M. *J. Am. Chem. Soc.* **1999**, *121*, 9208.
(34) Freeman, R. G.; Grabar, K. C.; Allison, K. J.; Bright, R. M.; Davis, J. A.; Guthrie, A. P.; Hommer, M. B.; Jackson, M. A.; Smith, P. C.; Walter, D. G.; Natan, M. J. *Science* **1995**, *267*, 1629.
(35) Novoselov, K. S.; Geim, A. K.; Morozov, S. V.; Jiang, D.; Zhang, Y.; Dubonos, S. V.; Grigorieva, I. V.; Firsov, A. A. *Science* **2004**, *306*, 666.
(36) Blake, P.; Hill, E. W.; Neto, A. H. C.; Novoselov, K. S.; Jiang, D.; Yang, R.; Booth, T. J.; Geim, A. K. *Appl. Phys. Lett.* **2007**, *91*, No. 063124.
(37) Abergel, D. S. L.; Russell, A.; Fal'ko, V. I. *Appl. Phys. Lett.* **2007**, *91*, No. 063125−3.

DOI: 10.1021/nl903414x | *Nano Lett.* **2010,** *10,* 553-561

(38) Casiraghi, C.; Hartschuh, A.; Lidorikis, E.; Qian, H.; Harutyunyan, H.; Gokus, T.; Novoselov, K. S.; Ferrari, A. C. *Nano Lett.* **2007**, *7*, 2711.
(39) Mohanty, N.; Berry, V. *Nano Lett.* **2008**, *8*, 4469.
(40) Shan, C. S.; Yang, H. F.; Song, J. F.; Han, D. X.; Ivaska, A.; Niu, L. *Anal. Chem.* **2009**, *81*, 2378.
(41) Geim, A. K.; Novoselov, K. S. *Nat. Mater.* **2007**, *6*, 183.
(42) Service, R. F. *Science* **2009**, *324*, 875.
(43) Geim, A. K. *Science* **2009**, *324*, 1530.
(44) Schedin, F.; Geim, A. K.; Morozov, S. V.; Hill, E. W.; Blake, P.; Katsnelson, M. I.; Novoselov, K. S. *Nat. Mater.* **2007**, *6*, 652.
(45) Leenaerts, O.; Partoens, B.; Peeters, F. M. *Phys. Rev. B* **2008**, *77*, 125416.
(46) Berger, C.; Song, Z. M.; Li, T. B.; Li, X. B.; Ogbazghi, A. Y.; Feng, R.; Dai, Z. T.; Marchenkov, A. N.; Conrad, E. H.; First, P. N.; de Heer, W. A. *J. Phys. Chem. B* **2004**, *108*, 19912.
(47) Wang, X. R.; Ouyang, Y. J.; Li, X. L.; Wang, H. L.; Guo, J.; Dai, H. J. *Phys. Rev. Lett.* **2008**, *100*, 206803.
(48) Guinea, F.; Horovitz, B.; Le Doussal, P. *Solid State Commun.* **2009**, *149*, 1140.
(49) Bruna, M.; Borini, S. *Appl. Phys. Lett.* **2009**, *94*, No. 031901.
(50) Rana, F. *IEEE Trans. Nanotechnol.* **2008**, *7*, 91–99.
(51) Das, B.; Voggu, R.; Rout, C. S.; Rao, C. N. R. *Chem. Commun.* **2008**, 5155.
(52) Lu, Y. H.; Chen, W.; Feng, Y. P.; He, P. M. *J. Phys. Chem. B* **2009**, *113*, 2.
(53) Wehling, T. O.; Novoselov, K. S.; Morozov, S. V.; Vdovin, E. E.; Katsnelson, M. I.; Geim, A. K.; Lichtenstein, A. I. *Nano Lett.* **2008**, *8*, 173.
(54) Manna, A. K.; Pati, S. K. *Chem.—Asian J.* **2009**, *4*, 855.
(55) Xie, L. M.; Ling, X.; Fang, Y.; Zhang, J.; Liu, Z. F. *J. Am. Chem. Soc.* **2009**, *131*, 9890.
(56) Gorgoi, M.; Michaelis, W.; Kampen, T. U.; Schlettwein, D.; Zahn, D. R. T. *Appl. Surf. Sci.* **2004**, *234*, 138.
(57) Tackley, D. R.; Dent, G.; Smith, W. E. *Phys. Chem. Chem. Phys.* **2001**, *3*, 1419.
(58) Tackley, D. R.; Dent, G.; Smith, W. E. *Phys. Chem. Chem. Phys.* **2000,** *2*, 3949.
(59) Martinez, V. M.; Arbeloa, F. U.; Prieto, J. B.; Lopez, T. A.; Arbeloa, I. L. *Langmuir* **2004**, *20*, 5709.
(60) Alfredsson, Y.; Ahlund, J.; Nilson, K.; Kjeldgaard, L.; O'Shea, J. N.; Theobald, J.; Bao, Z.; Martensson, N.; Sandell, A.; Puglia, C.; Siegbahn, H. *Thin Solid Films* **2005**, *493*, 13.
(61) Yonehara, H.; Etori, H.; Engel, M. K.; Tsushima, M.; Ikeda, N.; Ohno, T.; Pac, C. *Chem. Mater.* **2001**, *13*, 1015.
(62) Kluson, P.; Drobek, M.; Kalaji, A.; Karaskova, M.; Rakusan, J. *Res. Chem. Intermed.* **2009**, *35*, 103.
(63) Guthmuller, J.; Champagne, B. *J. Phys. Chem. A* **2008**, *112*, 3215.
(64) Cho, H. S.; Jeong, D. H.; Cho, S.; Kim, D.; Matsuzaki, Y.; Tanaka, K.; Tsuda, A.; Osuka, A. *J. Am. Chem. Soc.* **2002**, *124*, 14642.
(65) Raja, C.; Ananthanarayanan, K.; Natarajan, P. *Eur. Polym. J.* **2006**, *42*, 495.
(66) Michaels, A. M.; Nirmal, M.; Brus, L. E. *J. Am. Chem. Soc.* **1999**, *121*, 9932.
(67) Kneipp, K.; Kneipp, H.; Itzkan, I.; Dasari, R. R.; Feld, M. S. *Chem. Rev.* **1999**, *99*, 2957.
(68) Ichii, T.; Hosokawa, Y.; Kobayashi, K.; Matsushige, K.; Yamada, H. *Appl. Phys. Lett.* **2009**, *94*, 133110.
(69) Uehara, Y.; Ushioda, S. *Appl. Phys. Lett.* **2005**, *86*, 181905.
(70) Humbert, C.; Volcke, C.; Sartenaer, Y.; Peremans, A.; Thiry, P. A.; Dreesen, L. *Surf. Sci.* **2006**, *600*, 3702.
(71) Sariciftci, N. S.; Heeger, A. J.; Krasevec, V.; Venturini, P.; Mihailovic, D.; Cao, Y.; Libert, J.; Bredas, J. L. *Synth. Met.* **1994**, *62*, 107.
(72) Wang, Y. Y.; Ni, Z. H.; Shen, Z. X.; Wang, H. M.; Wu, Y. H. *Appl. Phys. Lett.* **2008**, *92*, No. 043121.
(73) Datta, S. S.; Strachan, D. R.; Mele, E. J.; Johnson, A. T. C. *Nano Lett.* **2009**, *9*, 7.
(74) Zhang, X. X.; Bao, M.; Pan, N.; Zhang, Y. X.; Jiang, J. Z. *Chin. J. Chem.* **2004**, *22*, 325.
(75) Nikitin, P. I.; Beloglazov, A. A.; Valeiko, M. V.; Creighton, J. A.; Wright, J. D. *Rev. Sci. Instrum.* **1997**, *68*, 2554.
(76) Creighton, J. A. *Surf. Sci.* **1983**, *124*, 209.
(77) Moskovits, M.; Suh, J. S. *J. Phys. Chem.* **1988**, *92*, 6327.

DOI: 10.1021/nl903414x | *Nano Lett.* **2010,** *10,* 553-561